Ellipsometry of Passive Oxide Films on Nickel in Acidic Sulfate Solution

Masahede Iida and Toashiaki Ohtsuka*
Graduate School of Engineering, Hokkaido University
Kita-ku, Sapporo 060-8628 Japan

*Corresponding author
E-mail ohtsuka@elechem1-mc.eng.hokudai.ac.jp
TEL & FAX +81-11-706-6351

Abstract

Nickel passive film has been studied in acidic sulfate solutions at pH 2.3 and 3.3 by ellipsometry. During anodic passivation followed by cathodic reduction, the roughness increases with dissolution of nickel, being indicated by gradual decrease of reflectance. However, the ellipsometric parameters, Ψ (arctan of relative amplitude ratio) and Δ (relative retardation of phase), are relatively insensitive to the roughness increase. From the change of Ψ and Δ, $\delta\Psi$ and $\delta\Delta$, during the anodic passivation and reduction, thickness of the passive oxide film was estimated with assumption of refractive index of n_f = 2.3 of the film. The thickness estimated is a range between 1.4 and 1.7 nm in the passive potential region from 0.8 V to 1.4 V vs. RHE, having a tendency of thickening with increase of potential. Cathodic reduction at constant potential induces a change of the oxide film to an oxide film with lower refractive index of n_f = 1.7, accompanied by thickening of the film about 30 % more in the initial stage of reduction for 30 s. The gradual decrease of thickness takes place for the oxide with the lower refractive index in the latter stage. The potential change from the passive region to cathodic hydrogen evolution region may initially cause hydration of the passive oxide of NiO, ie., $NiO + H_2O = Ni(OH)_2$, and during the latter stage of reduction, the hydrated nickel oxide gradually dissolves.

Key Words; ellipsometry, nickel, passivation, oxide film, thickness

Introduction

Nickel is one of the typical passivation metals on which very thin oxide films covers, and the substrate metals are efficiently protected by the passive oxide films a few nm thick. The passive oxide film anodically formed on nickel was studied by various authors. Macdonald et al. claimed that the passive film consisted of the inner NiO of a barrier layer and outer $Ni(OH)_2$ porous or hydrated layer, in which the inner layer behaves as a p-type oxide with cation vacancy. [1,2] Oblonsky and Devine measured surface enhanced Raman spectra of nickel passivated in neutral borate solution and estimated amorphous $Ni(OH)_2$ in passive potential region and NiOOH in the higher transpassive region. [3] Further, the passive film formed in acidic and neutral solution was assumed to be a partially hydrated NiO by various authors. [4-11] The anodic film formed in alkaline solution was assumed to be $Ni(OH)_2$ in the passive region and NiOOH in the high potentials close to oxygen evolution potential. The films in the alkaline solution were supposed to be much thicker than those in neutral solution. [12-14] The both passive films formed in neutral and alkaline solutions were found to be p-type semiconductor from the Mott-Schottky plot of the capacitance data. [1, 2, 15, 16]

The thickness of the passive film has been measured by using ellipsometry. Kudo et al. applied it to the passive film on nickel in neutral borate solution and estimated 0.7-1.5 nm thickness dependent on anodic potential. [10] A similar results were reported by Paik and Szklarska-Simialowska. [6] In acidic aqueous solution, the thickness measurement was much restricted, because the high anodic dissolution in the acidic solution induces a rough surface which interferes with precise determination of the thickness of the surface oxide. Ohtsuka et al. estimated the thickness and optical properties of nickel passive oxide film in acidic sulfate solution by reflectance measurement of polarized lights. [7-9] They reported that the film thickness was about 1.5- 2.0 nm and the refractive index depended on anodic potential. Kang and Paik measured by ellipsometry combined with reflectance the initial passive film in acidic sulfate solution. [5] They reported that the complex refractive index of the film depended on potential and oxidation time, and the thickness after 60 s oxidation reach 1.2 nm at a potential of 0.9 V vs SCE.

In this paper, we apply ellipsometry to the passive film on nickel in acidic

sulfate solutions at pH 2.3 and 3.3. We estimated the thickness of the passive film on roughening surface from the change of ellipsometric parameters during cathodic reduction following anodic passivation. It was found that the thickness of the passive film was about 1.4-1.7 nm and cathodic polarization introduced hydration of the passive film.

Experimental

The electrode used was nickel sheet 99.99% pure with dimension 10x 10 x 1 mm with a small handle. It was mechanically polished to mirror-like surface using alumina abrasive down to 0.05 μm diameter and then ultrasonically washed in acetone before experiments.

The electrolytes were 0.1 mol dm^{-3} (M) sulfuric acid solution and mixtures of 0.1 M sulfuric acid solution and 0.1 M sodium sulfate solution at pH 2.3 and 3.3. They were prepared from analytical grade reagents and milli-Q pure water, and deaerated by nitrogen bubbling for 2 h before experiments.

The ellipsometer and the optical-electrochemical cell were previously described. [17] The ellipsometer was an automated rotating analyzer apparatus designed by authors, in which the ellipsometric parameters, Ψ and Δ, and reflectance, R, were simultaneously monitored in 1 s interval. The angle of incidence was 60.0 degree and the light with 632.8 nm wavelength from a He-Ne stabilized laser was used. The potentials were measured vs. reference electrode of Ag/AgCl/ saturated KCl and converted to potentials vs. the reversible hydrogen electrode in the same solution (RHE).

The ellipsometric measurement was started with galvanostatic reduction at 20 μA cm^{-2} in 0.1 M sulfuric acid solution for 900 s to remove the air-formed oxide film. After change of the solution to acidic sulfate solution at pH 2.3 or 3.3, the potentials were shifted as the following way; -0.097 V vs. RHE at the pH 2.3 solution or to –0.108 V vs. RHE at the pH 3.3 solution for the reduction, then an anodic passive potential between 0.51 and 1.41 V for 800 s, followed by cathodic potential same as the initial for 3700 s. The ellipsometric measurement was done with current monitoring during the potential shift.

Results

Thickness of passive oxide film

Nickel electrode reveals a typical passivation phenomenon in the acidic sulfate solutions. Figure 1 shows a potential-current density (CD) relation, in which the CD was taken after 800 s polarization at individual potentials. In the passive potential region starting from about 0.4 V vs. RHE, the CD is kept at a few μA cm^{-2}. The CD rises from 1.2 V, corresponding to transpassive dissolution.

Figure 2 shows an example of ellipsometric measurement, in which the oxidation was made at 0.81 V vs. RHE in the pH 2.3 sulfate solution after reduction at –0.097 V. In Fig. 1(A), relative reflectance, $\Delta R/R_0 = (R-R_0)/R_0$, and CD are platted, where R_0 is reflectance at the initial reduced surface at –0.097 V. In Fig. 2(B), changes of ellipsometric parameters, Ψ and Δ, are shown, in which Ψ and Δ are, respectively, relative amplitude ratio of perpendicular polarized (s-polarized) light to parallel polarized (p-polarized) light and relative phase retardation between p- and s-polarized lights. The reflectance continuously decreases with time regardless of polarization except for the initial large change at the oxidation at 0.81 V. The continuous decrease of reflectance may reflect gradual roughening of surface and the abrupt decrease at the initial at 0.81 V may be induced by a large dissolution at the initial oxidation from the reduced bare surface. The ellipsometric parameters are not so large change in comparison with the reflectance. However, the parameters after the reduction at –0,097 V for 3700 s do not recover to the initial values. From Ψ_0 = 33.7 degree and Δ_0 = 138.5 degree for the initial reduced surface, the complex refractive index of substrate nickel is calculated to be N_S = 2.58 – j3.86. The gradual roughening surface may change the apparent refractive index of the substrate with time. Although the large change occurs for reflectance during the oxidation-reduction cycle, Ψ and Δ do not greatly change. The difference between the initial and final reduced surface was $\delta\Psi$ = 0.17 degree and $\delta\Delta$ = -0.55 degree which meant the apparent refractive index changed from N_S = 2.58 – j3.86 to N_S = 2.51 – j3.85. The ellispsometric parameters are supposed to be less sensitive to the roughness change of surface than reflectance.

For estimation of the film thickness, since the effect of roughness change on the change of ellipsometric parameters should be canceled, we adopt the values of the final reduced surface as the parameters corresponding to the bare surface for calculation. Figure 3 shows difference of the ellipsometric parameters, $\delta\Psi$ and $\delta\Delta$,

from the surface covered by the oxide film at individual potentials to the final reduced surface. The change of Δ tends to increase with potential, however, the change of Ψ is so small between 0.1 and 0.2 degree that one may not distinguish the dependence on potential. In potentials lower than 0.8 V, since the roughness change was thought to be large from the reflectance change during the oxidation, the data was excluded from the plot.

The calculation of the thickness of the oxide film is started from the complex refractive index of the bare surface. For the bare surface, complex refractive index of N_S = 2.58 – j3.86 is used, which was calculated from Ψ_0 = 33.7 degree and Δ_0 = 138.5 degree, of the first reduced surface. Figure 4 indicates plot of $\delta\Psi$ vs. $\delta\Delta$ for the oxide film in comparison with the theoretical relation of growing films as a parameter of complex refractive index and thickness of the film. In Fig. 4, we assumed a refractive index of n_f = 2.3 for nickel oxide film. From the comparison, it is seen that the film thickness is in the range between 1.3 and 1.7 nm.

In Fig. 5, the film thickness estimated from the comparison in Fig.4 is described as a function of potential. In Fig. 5, the CDs taken after 800 s polarization at the individual potential are plotted in logarithmic scale. The thickness which is conceivable to be not dpendent on the solution pH tends to slight increase with increase of potential.

Reduction of passive oxide film

The passive oxide film may cathodically be removed from the surface during constant potential reduction following the anodic passivation. Fig. 6 shows CD transient during the reduction at –0.097 V in the pH 2.3 sulfate solution after the oxidation at various potentials. The CD reveals an initial cathodic spike, then decreasing gradually with time. The initial spike of CD is smaller with the higher potential of formation of passive film. The change of $\delta\Delta$ and $\delta\Psi$ during the reduction is shown in Fig. 7, in which the passive film formed at 0.81 V or 1.11 V is gradually attenuated during the reduction at –0.097 V in the pH 2.3 sulfate solution. The $\delta\Delta$ greatly increases at the initial stage, then gradually approaching to $\delta\Delta = 0$ correspondent to the bare surface. The $\delta\Psi$ sharply increases at the initial 20 s during the reduction, however, the direction of $\delta\Psi$ changes to negative for the film formed at 1.11 V, after $\delta\Psi$ reveals a maximum. In Fig. 8 experimental loci of $\delta\Psi$ vs. $\delta\Delta$ is

shown during the reduction of the passive film formed at 1.11 V in the pH 2.3 sulfate solution. When one compared the loci with simulated relation between $\delta\Psi$ and $\delta\Delta$ as a function of complex refractive index and film thickness, it is found that the film initially changes to a film having a lower refractive index of about n_f = 1.7. In Fig.8 the simulated loci calculated from a homogeneous layer model are plotted as comparison.

The change of the film thickness during the reduction at –0.097 V of the film formed at 1.11 V in the pH 2.3 sulfate solution was evaluated. The result is given in Fig. 9, in which the initial passive film with complex refractive index of N = 2.3 – j0.389 is changed to the film with index to N = 1.7 – j0.023 during the reduction. The passive film thickens with time during the initial reduction, accompanied by the change of refractive index of the film at n = 2.3 to 1.7. After reaching a maximum thickness of about 2.4 nm, the thickness gradually decreases with time.

In Fig. 10, the change of the thickness of the films formed in the pH 3.3 sulfate solution at various potentials during the constant potential reduction at –0.108 V. In Fig. 10 (A), the thickness changes are plotted at the initial stage of the reduction and in Fig. 10 (B), they are plotted during the overall stage to complete reduction. The film reveals a maximum thickness at reduction for about 30 s, then decreasing with time to d = 0 nm.

Discussion

Thickness of Passive Film

As shown in Fig. 5, the thickness of the passive film on nickel does not reveal clear dependence of the formation potential in acidic sulfate solution. It does not also have clear pH dependence. The similar result on the thickness- potential relation was reported in the previous paper by reflectance measurement. [8]

For the passive oxide film on iron, the thickness was reported to linearly increase with potential and the stationary current density through the passive film independent of potential was a linear function of solution pH. The relation was interpreted by Vetter et al. [18, 19] and Sato et al. [20] from the high-field ionic migration model through the passive film proposed by Cabrera and Mott [21] and from a potential difference at the oxide/ solution interface, at which the O^{2-} or OH^- on the oxide film was in equilibrium with H_2O in aqueous solution phase.

$O^{2-}(ox) + 2H^{+}(soln) = H_2O(soln)$ (A)

From the equilibrium of the reaction, the interfacial potential difference is a function of solution pH and independent of potential.

$E(ox/\ soln) = E^0(ox/\ soln) - 2.303\ (RT/\ F)\ pH$ (1)

Since the interfacial potential is constant independent of anodic bias, the potential difference through the oxide film is linearly proportional to anodic bias. The film thickness followed by the high-field ionic migration model results in linear relation to the anodic bias.

For nickel passivation film, interfacial potential difference at the passive oxide film/ solution interface may not be constant and depends on anodic bias. Nickel passive oxide has been proposed to be composed of NiO, [8, 10, 11] in which the cation vacancy concentration and positive hole have been conservable to be an important factor for determination of the interfacial potential difference. Real composition of NiO is described as a cation-deficient oxide of $Ni_{1-x}O$, where the nonstoichiometry, x, is dependent on the oxygen partial pressure. The oxygen pressure of the oxide surface could be described as a function of anodic bias.

$2H_2O(soln) = 4H^{+}(soln) + O_2(ox) + 4e(Ni)$ (B)

where (soln) indicates aqueous solution phase, (ox) oxide phase, and (Ni) nickel substrate. Since one assumes an electrochemical equilibrium between electrons of oxide surface and nickel substrate, the interfacial pressure of oxygen exponentially increases with anodic bias. The oxygen gas pressure is equilibrated with concentration of defect of cation vacancies, V_{Ni}, on the oxide surface

$O_2\ (ox) = 2V_{Ni}''(ox) + 4h(ox) + 2O_O^{x}$ (2)

Overall, the V_{Ni}'' may be described as the following.

$2H_2O(soln) = 2V_{Ni}''(ox) + 4e(Ni) + 4h(ox) + 2O_O^{x}(ox) + 4H^{+}(soln)$ (C)

where V_{Ni}'' indicates a cationic vacancy with –2 valence, h a positive hole, and O_O^{x} an oxygen ion in the regular lattice site. Since the chemical potential of positive hole equals to negative chemical potential of electron, $\mu_h = -\mu_e$, the following equation should be held for the equilibrium of the above reaction.

$2\mu_{H2O} = (2\mu_{VNi''} + 2\mu_{OO}^{x} + 4\mu_{H+}) - 4F(\phi_{ox} - \phi_{soln})$ (3)

where μ_i indicates chemical potential of *i* species. Since the interfacial potential difference at the oxide/ solution interface, $E(ox/\ soln) = \phi_{ox} - \phi_{soln}$,

$E(ox/\ soln) = -\ (1/2F)\ [\mu_{H2O} - (\mu_{VNi''} + \mu_{OO}^{x} + 2\mu_{H+})$

$$= E^0(\text{ox/ soln}) + (RT/2F) \ln a_{VNi+} - (RT/F)(2.303)\, pH \qquad (4)$$

Accordingly the interfacial potential difference for nickel passivation is found to be a function of activity or concentration of cationic vacancy. Since the vacancy concentration increases with oxygen partial pressure or anodic bias, the interfacial potential difference is also increased with anodic bias. Although the potential difference through the oxide film linearly increases with anodic bias for iron passivation, it is not directly proportional to anodic bias for nickel passivation, because the interfacial potential difference increases with anodic bias. The vacancy concentration increased with anodic bias is expected to enhance ionic migration through the oxide film and the interfacial ionic transfer. The increase of stationary CD has been observed as the transpassive dissolution of nickel in the higher potential region. [10] Since the film thickness is assumed to be determined by the potential difference through the oxide film and ionic migration rate, both of which is a function of cation vacancy concentration increased with anodic bias, the thickness-potential relation is not easily evaluated from the simulation. Cancellation of the partial increase of the potential difference through the oxide film and the increase of rate of ionic migration rate i.e., migration rate of cation vacancy with anodic bias may result in almost constant thickness independent of anodic bias.

Cathodic reduction of nickel passive film

When the abrupt potential change is made from anodic potential in the passive region to cathodic in the hydrogen evolution region, the change of refractive index initially takes place, followed by thinning of the oxide film, as shown in Figs. 9 and 10. The decrease of refractive index of the film during the initial stage of reduction was also reported in the previous paper by reflectance measurement. [8, 22] The decrease of the refractive index may be explained by hydration of the passive oxide. When one assumes that the passive oxide film is composed of NiO, the initial reaction may be hydration of the passive oxide film in addition to reduction from NiO and metallic Ni.

$$NiO + H_2O = Ni(OH)_2 \qquad (C)$$

$$NiO + 2H^+ + 2e = Ni + H_2O \qquad (D)$$

The hydration of the oxide film in the cathodic potential and the dehydration in the passive potential was also presumed by Kim and Seo from stress measurement of

passive nickel electrode in neutral solution. [23] Dehydration and hydration processes of the thin oxide film may originate in the electric field in the film. When the electric field is enough high, the dehydration takes place, and when the field is removed, the hydration takes place inversely. Two origins of dehydration induced by the electric field may be considered. (1) The electroosomotic flow under the high field through extremely thin channels in the oxide film is accompanied by movement of water molecules. (2) The secondary Wien effect or field dissociation effect induces a change of the equilibrium constant of the following de-protonation reaction.

$$\text{Ni-O-H} = \text{NiO}^- + \text{H}^+ \qquad \text{(E)}$$

$$K = a_{(\text{Ni-O-})}\, a_{(\text{H+})} / a_{(\text{Ni-OH})} \qquad (5)$$

Since the field dissociation effect is proposed to be caused by a field of 10^5 V cm^{-1} order, the electric field which has been estimated to be 10^6 V cm^{-1} in the oxide film from the thickness- potential relation can induce this dissociation change.

The cathodic process to reduce the passive oxide film may be summarized by the following way. The passive oxide film of NiO is hydrated in addition to reduction metallic Ni in the initial stage for 30 s after potential change from the anodic passive region to the cathodic hydrogen evolution region. Then the hydrated nickel oxide of $Ni(OH)_2$ gradually dissolves to Ni^{2+} or reduced to metallic nickel.

Conclusion

The thickness of passive oxide film on nickel formed in acidic sulfate solutions at pH 2.3 and 3.3 was evaluated by ellipsometry.

(1) The thickness estimated is a range between 1.4 and 1.7 nm in the passive potential region from 0.8 V to 1.4 V vs. RHE, having a tendency of slight thickening with increase of potential.
(2) Cathodic reduction at constant potential initially induces a change of the passive oxide film to an oxide film with lower refractive index of $n_f = 1.7$. The decrease of the refractive index may be explained by hydration of the passive oxide from NiO to $Ni(OH)_2$. The hydrated nickel oxide, $Ni(OH)_2$, gradually dissolves during the latter stage of reduction.

References

(1) E. Sikora, D. D. Macdonald, Electrochim. Acta, 48 (2002) 69.

(2) D. D. Macdonald, S. Smedley, 35 (1990) 1949.

(3) L. J. Oblonsky, T. M. Devine, J. Electrochem. Soc., 142 (1995) 3677.

(4) S. C. Tjong, Mat. Res. Bull., 17 (1982) 1297.

(5) Y. Kang, W.-K. Paik, Surface Sci., 182 (2987) 257.

(6) W.-K. Paik, Z. Szklarska-Simialowska, Surface Sci., 96 (1980) 401.

(7) T. Ohtsuka, K. Schoner, K. E. Heusler, J. Electroanal. Chem., 93 (1978) 171.

(8) T. Ohtsuka, K. E. Heusler, J. Electroanal. Chem., 100 (1979) 319.

(9) K. E. Heusler, T. Ohtsuka, Surface Sci., 101 (1980) 194.

(10) N. Sato, K. Kudo, Electrocheim. Acta, 19 (1974) 461.

(11) B. Macdougall, D, F, Mitchel, M. J. Graham, Corrosion, 38 (1982) 85.

(12) J. O. Zerbino, C. De Pauli, D. posadas, A. J. Arvia, J. Electroanal. Chem., 330 (1992) 675.

(13) L. M. M. de Souza, F. P. Kong, F. R. McLarnon, R. H. Muller, Electrochim. Acta, 42 (1997) 1253.

(14) F. Kong, R. Kostecki, F. Mclarnon, R. H. Muller, Thin Solid Films, 314-314 (1998) 775.

(15) K. Darowicki, S. Krolowiak, P. Slepski, Electrochem. Acta, 51 (2006) 2204; Mott-Schottky plot, 0.1M NaOH.

(16) S. Maximovitch, Electrochim. Acta, 41 (1996) 2761.

(17) T. Ohtsuka, Y. Sato, K. Uosaki, Langmuir, 10 (1994) 3658.

(18) K. J. Vetter, F. Gorn, Electrochim. Acta, 18 (1973) 1090

(19) K. J. Vetter, F. Gorn, Werkst. u. Korrosion, 21 (1973) 703.

(20) N. Sato and T. Noda, Electrochim. Acta, 22 (1977) 839.

(21) H. Cabrera, N. F. Mott, Rep. Progr. Phys., 12 (1949) 163.

(22) T. Ohtsuka and K. E. Heusler, 102 (1979) 175.

(23) J.-D. Kim and M. Seo, J. Electrochem. Soc., 150 (2003) B193.

Figure Caption

Figure 1 Current density (CD) vs. potential relation. CD was taken after 800 s polarization at individual potentials.

Figure 2 Change of CD, reflectance, and ellipsometric parameters, Ψ and Δ during reduction- passivation- reduction cycle in the pH 2.3 sulfate solution. The initial reduction was made at –0.097 V for 360 s following reduction at constant CD of 20 mA cm^{-2} in 0.1 M H_2SO_4. The passivation was made at 0.81 V for 800 s followed by the reduction at -0.097 V for 3700 s. (A) CD and relative reflectivity, dR/R_0, (B) Ψ and Δ.

Figure 3 Change of Ψ and Δ during the reduction of the passive oxide film formed at various potentials in the pH 2.3 and 3.3 sulfate solutions.

Figure 4 $\delta\Delta$-$\delta\Psi$ plot for the passive oxide film. The simulation curves were superimposed as a parameter of film thickness with assumption of n_f = 2.3.

Figure 5 Film thickness as a function of potential. CD was also plotted in logarithmic scale.

Figure 6 Transient of cathodic CD during the reduction at –0.097 V in the pH 2.3 sulfate solution for the passive film formed at various potentials.

Figure 7 Change of Ψ and Δ during the reduction at –0.097 V in in the pH 2.3 sulfate solution for the passive film formed at potentials of 0.81 V and 1.11 V

Figure 8 Change of $\delta\Delta$-$\delta\Psi$ loci during the reduction at –0.097 V in the pH 2.3 sulfate solution for the passive film formed at potential of 1.11 V. The simulation curves were superimposed as a parameter of film thickness with assumption of N_f = 2.3 –j0.389 for the passive film and of N_f = 1.7 – j0.023 for the reduced oxide.

Figure 9 Change of refractive index and thickness during the reduction at –0.097 V in

the pH 2.3 sulfate solution for the passive film formed at potential of 1.11 V.

Figure 10 Change of thickness during the reduction at –0.108 V in the pH 3.3 sulfate solution for the passive film formed at potentials of 0.91, 1.11, and 1.31 V.

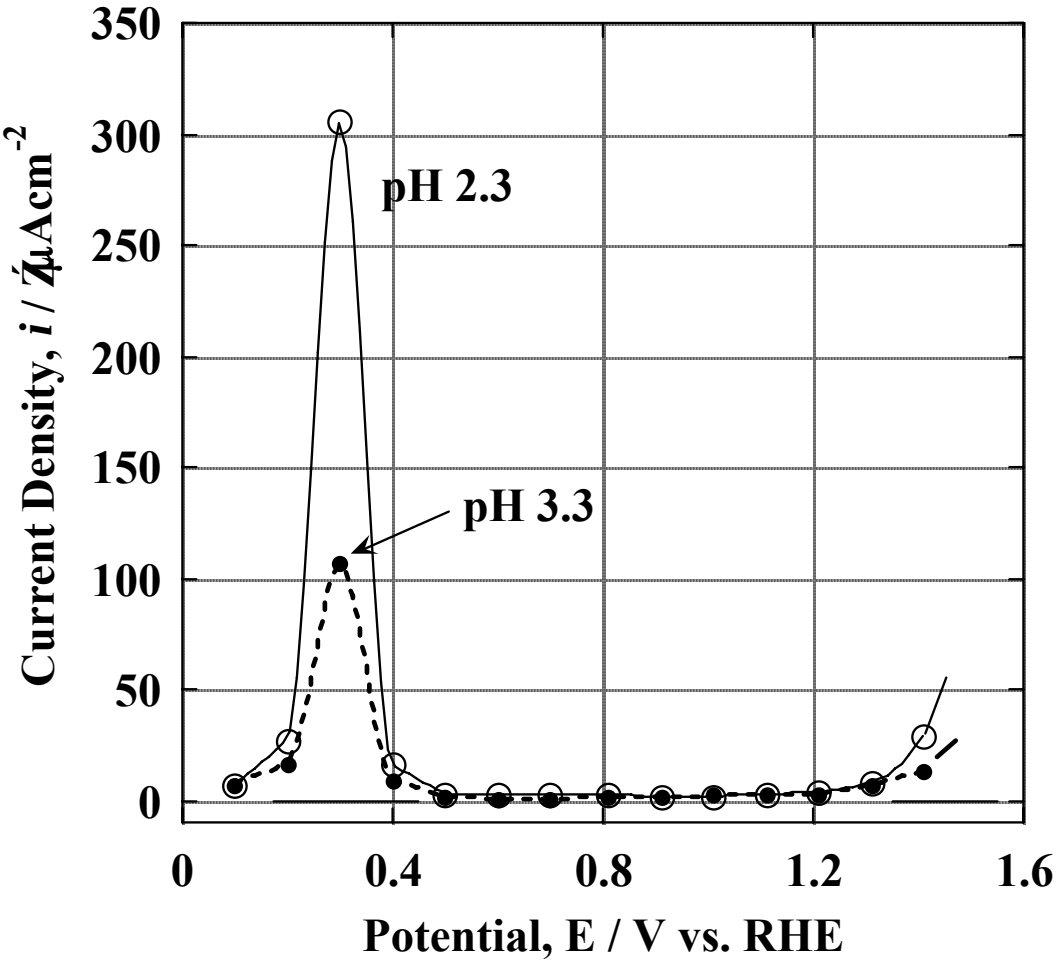

Figure 1 Current density (CD) vs. potential relation. CD was taken after 800 s polarization at individual potentials.

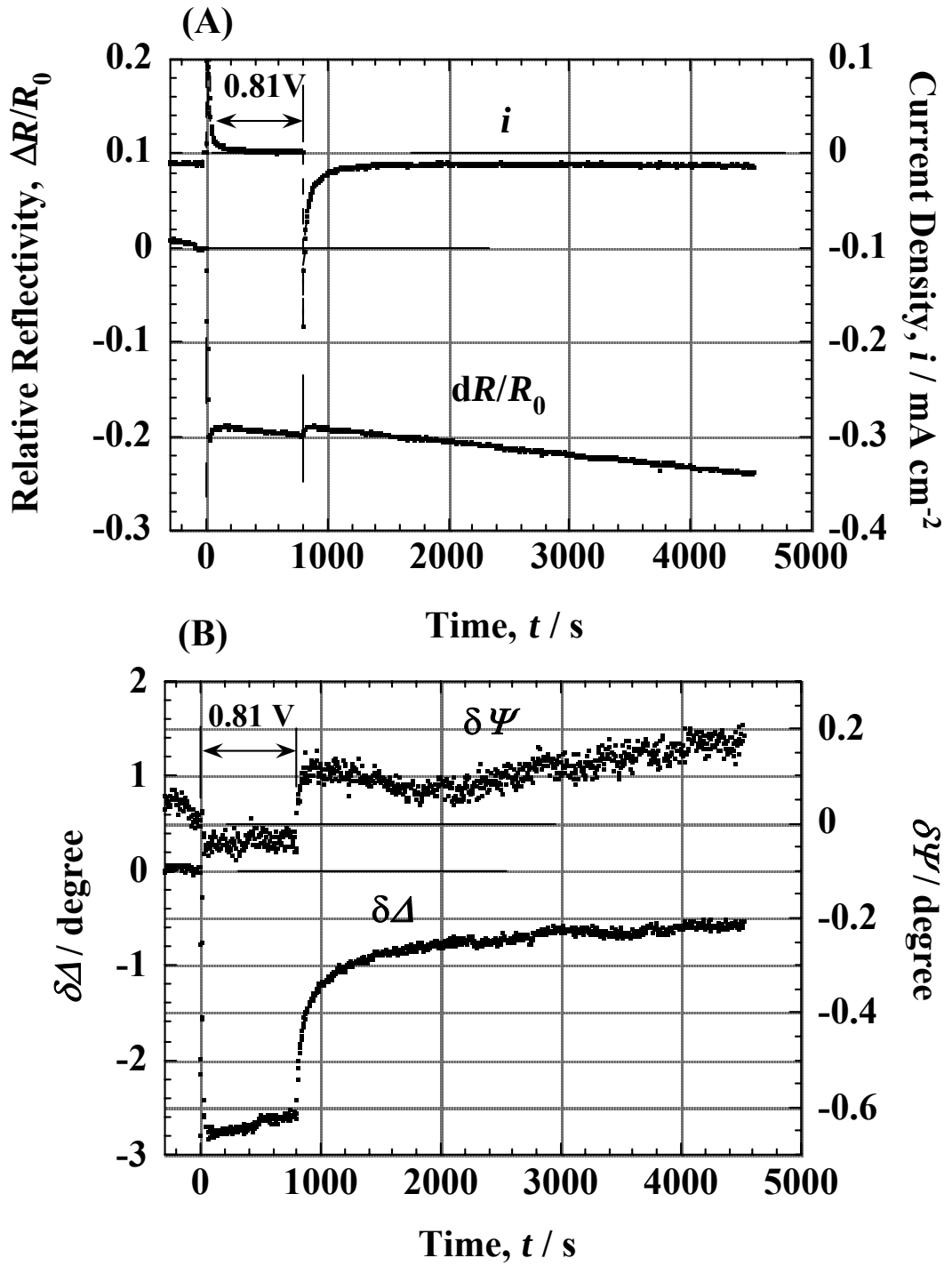

Figure 2 Change of CD, reflectance, and ellipsometric parameters, Ψ and Δ during reduction- passivation- reduction cycle in the pH 2.3 sulfate solution. The initial reduction was made at –0.097 V for 360 s following reduction at constant CD of 20 mA cm^{-2} in 0.1 M H_2SO_4. The passivation was made at 0.81 V for 800 s followed by the reduction at -0.097 V for 3700 s. (A) CD and relative reflectivity, dR/R_0, (B) Ψ and Δ.

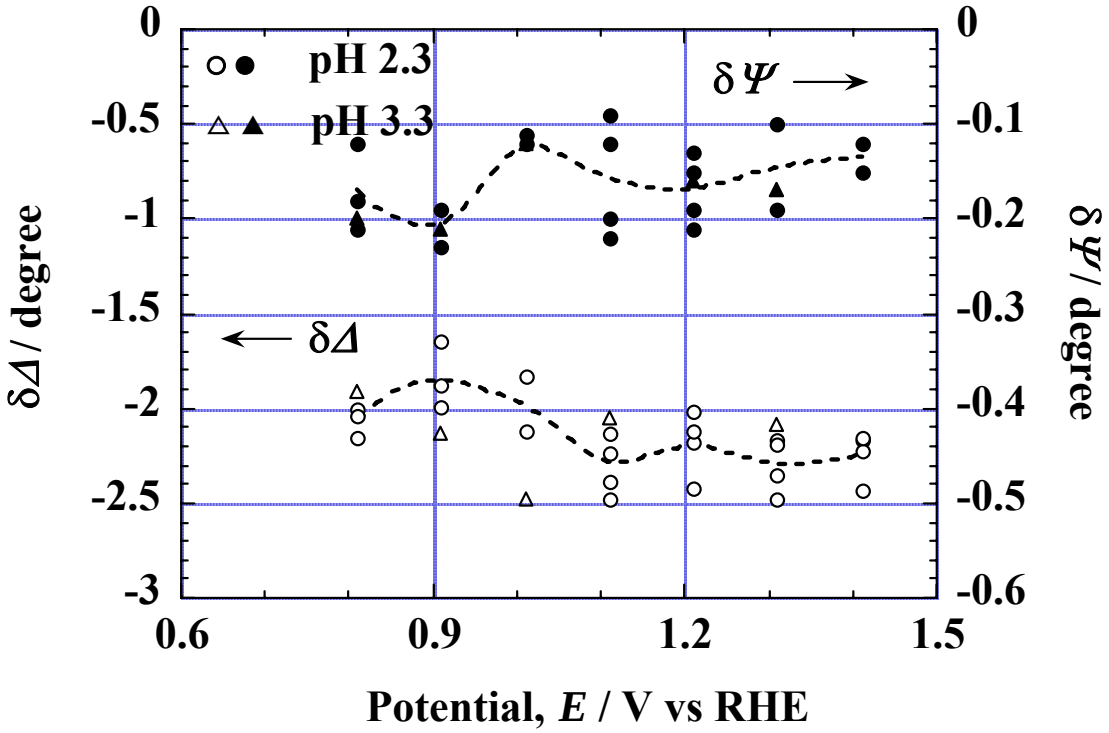

Figure 3 Change of Ψ and Δ during the reduction of the passive oxide film formed at various potentials in the pH 2.3 and 3.3 sulfate solutions.

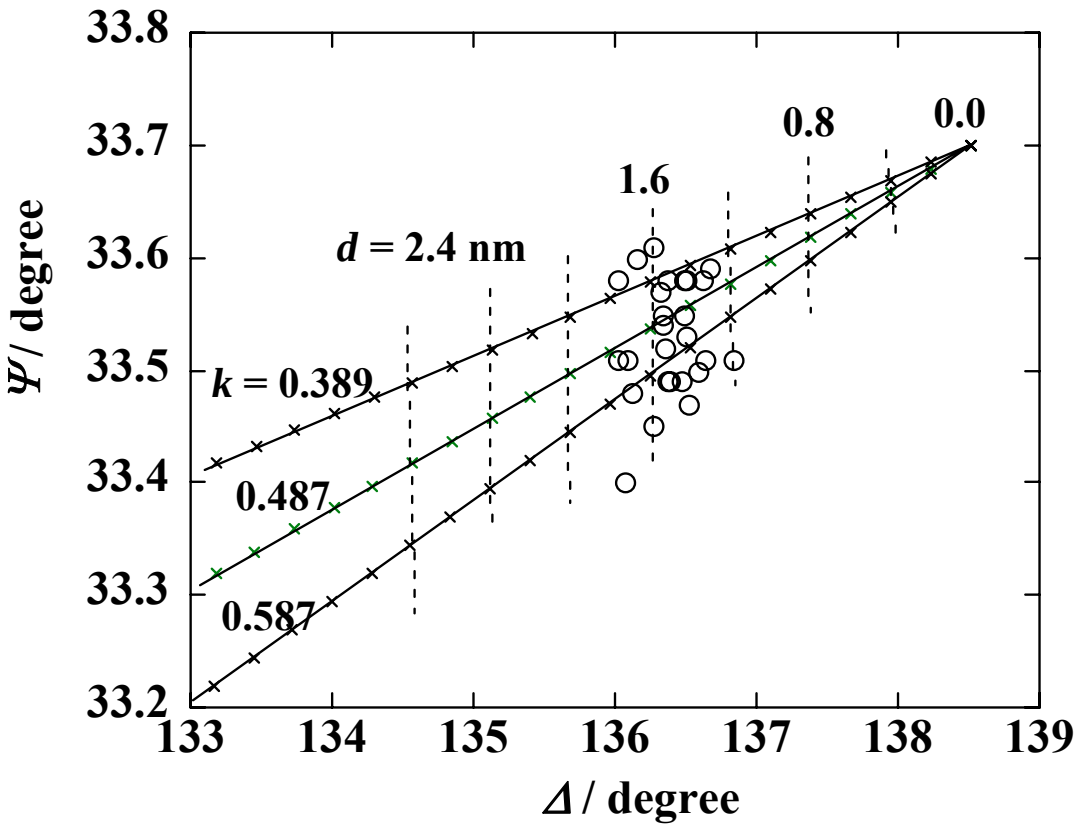

Figure 4 $\delta\Delta$-$\delta\Psi$ plot for the passive oxide film. The simulation curves were superimposed as a parameter of film thickness with assumption of $n_f = 2.3$.

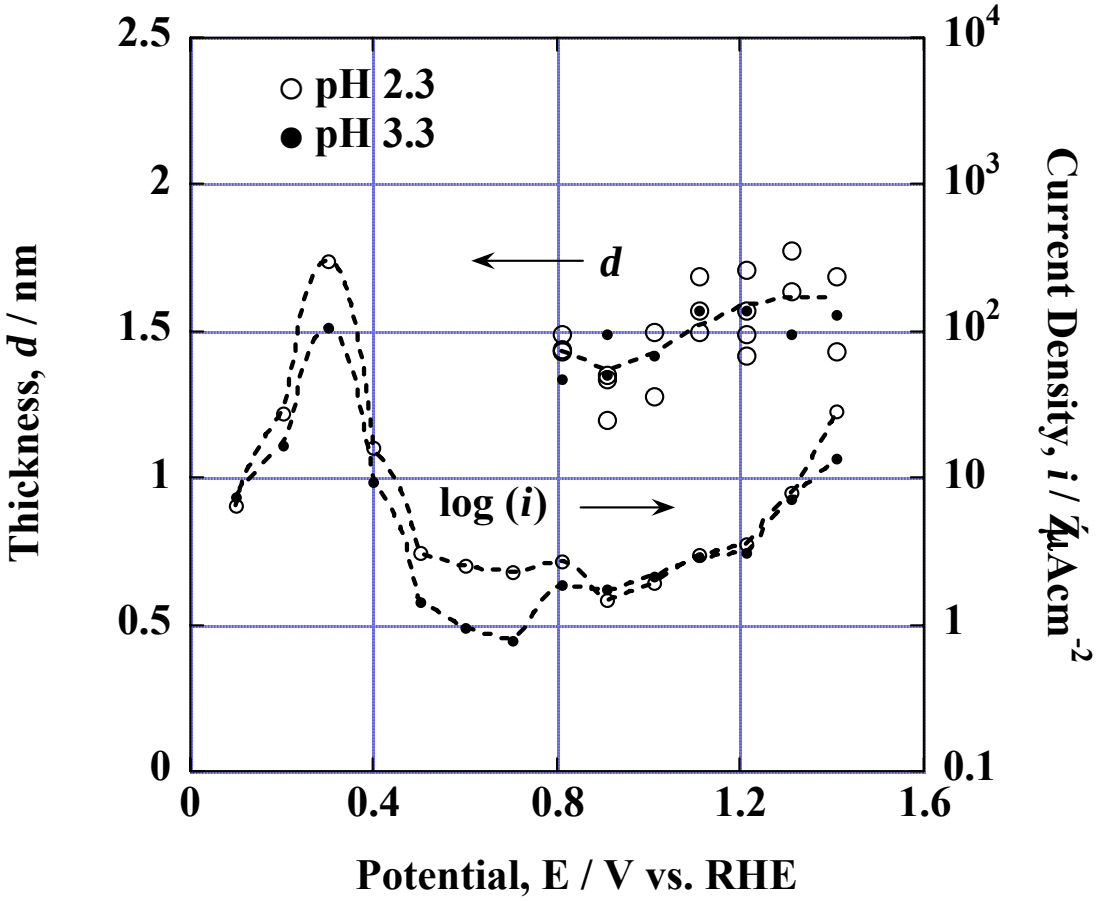

Figure 5 Film thickness as a function of potential. CD was also plotted in logarithmic scale.

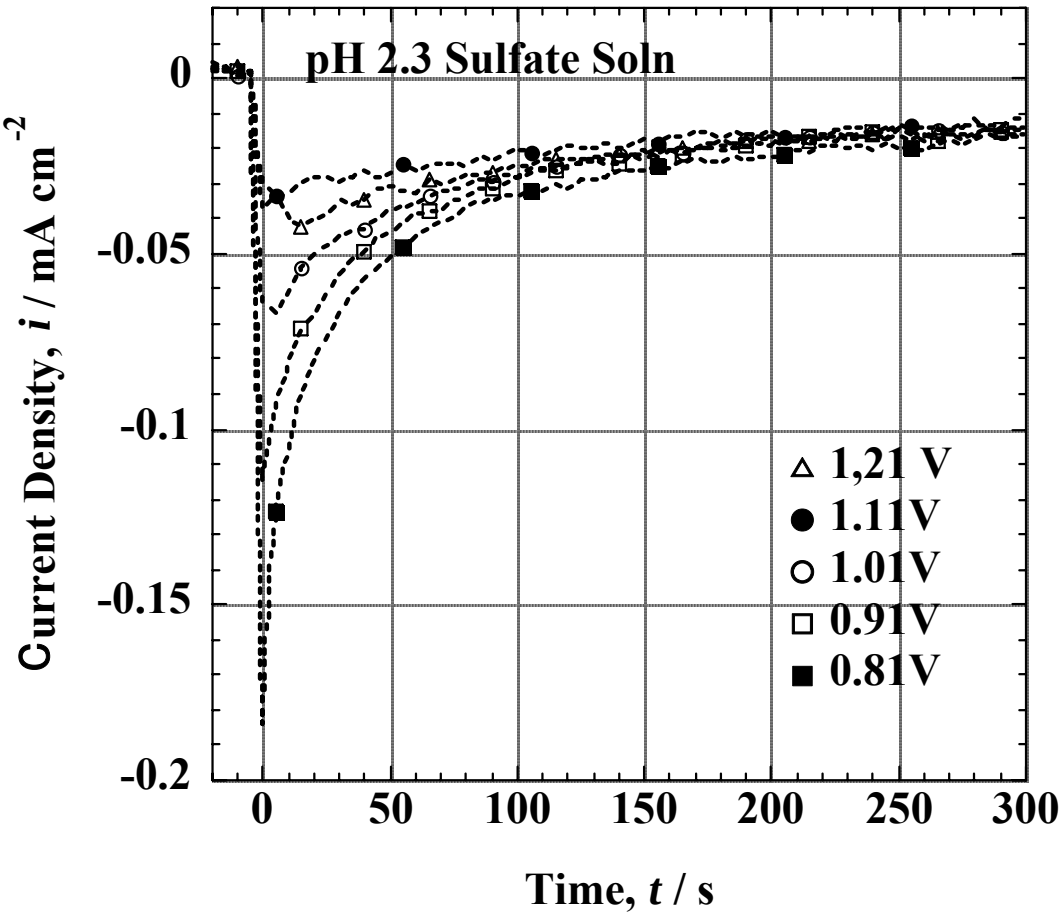

Figure 6 Transient of cathodic CD during the reduction at –0.097 V in the pH 2.3 sulfate solution for the passive film formed at various potentials.

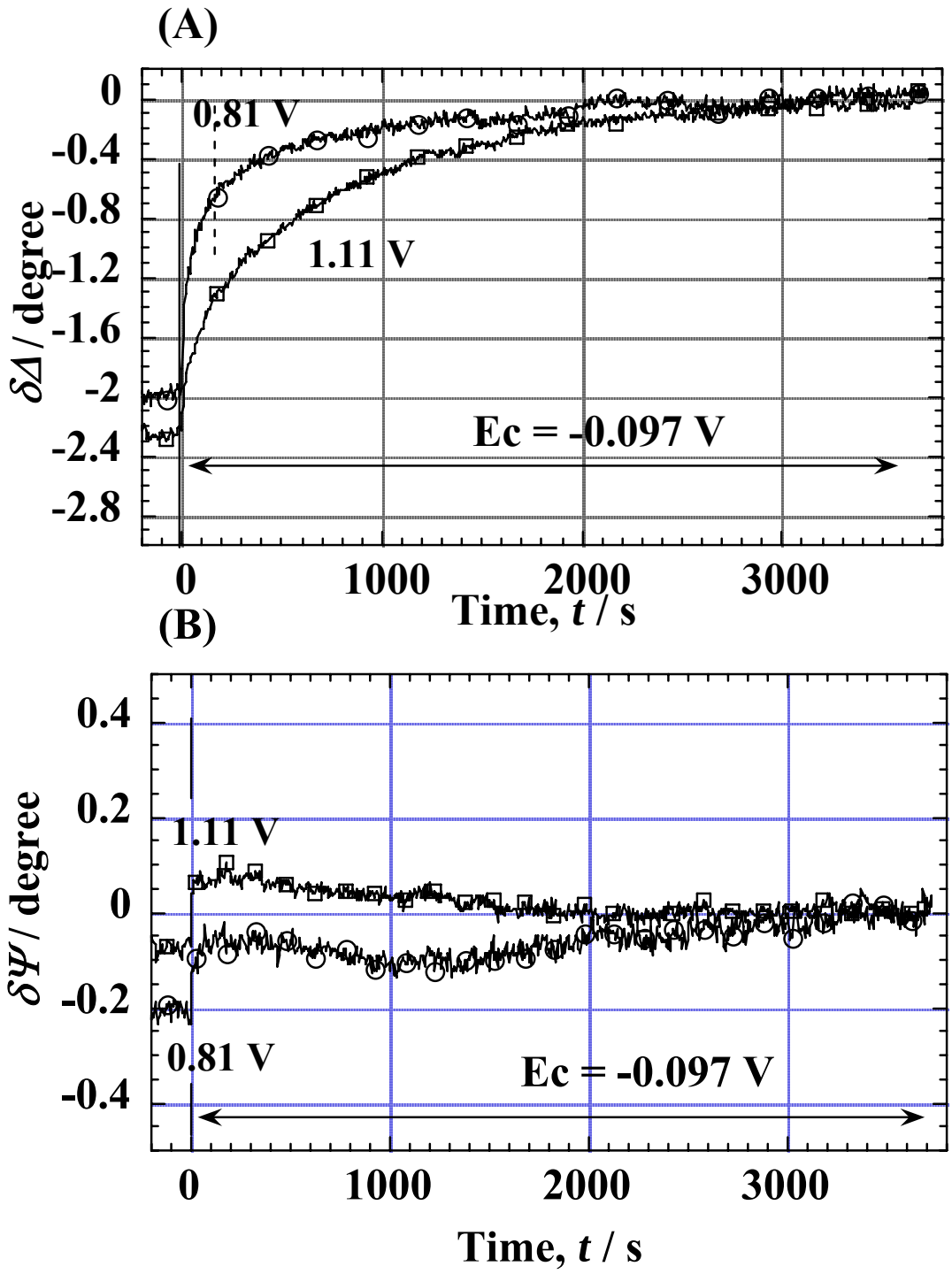

Figure 7 Change of Ψ and Δ during the reduction at –0.097 V in in the pH 2.3 sulfate solution for the passive film formed at potentials of 0.81 V and 1.11 V

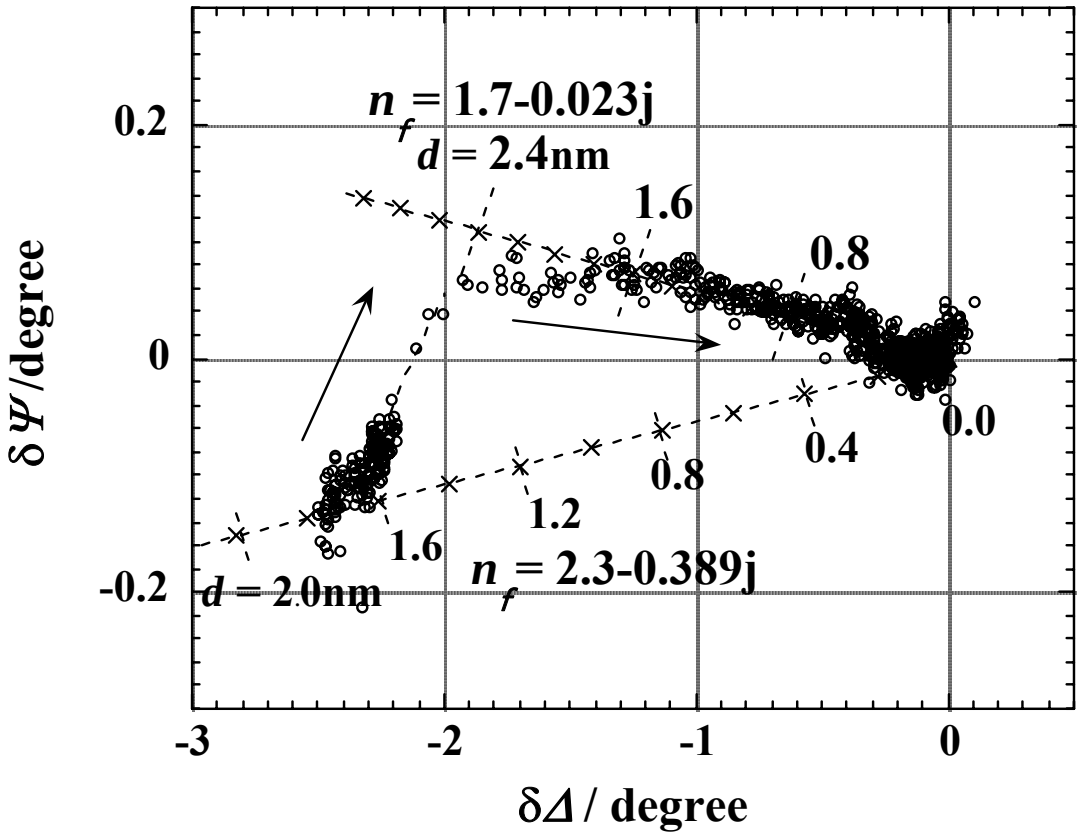

Figure 8 Change of $\delta\Delta$-$\delta\Psi$ loci during the reduction at –0.097 V in the pH 2.3 sulfate solution for the passive film formed at potential of 1.11 V. The simulation curves were superimposed as a parameter of film thickness with assumption of N_f = 2.3 –j0.389 for the passive film and of N_f = 1.7 – j0.023 for the reduced oxide.

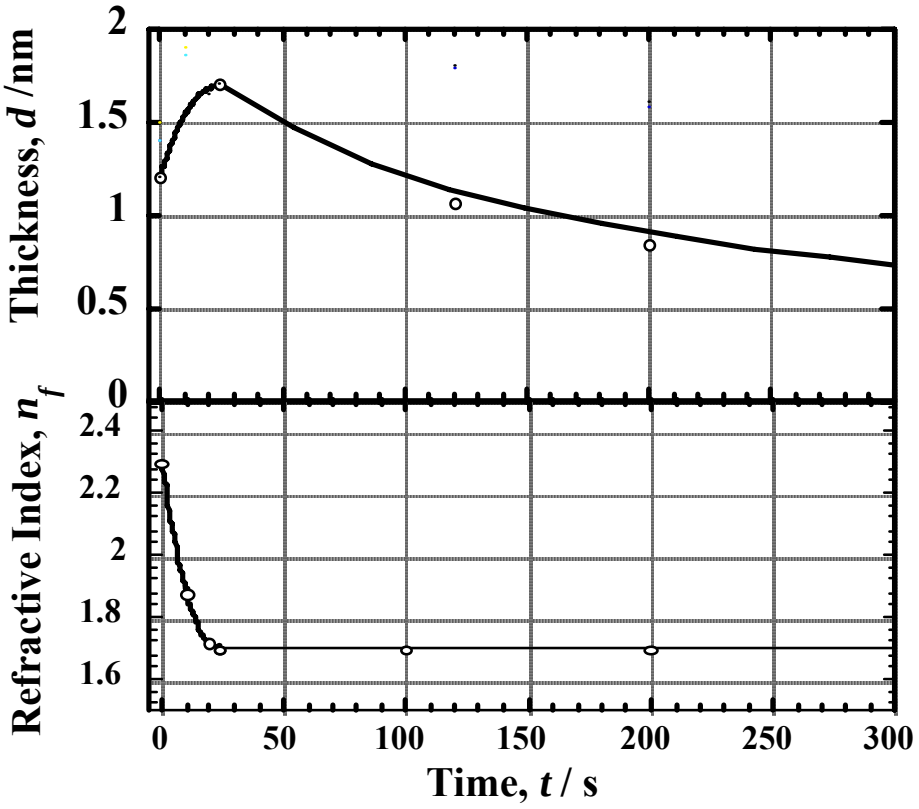

Figure 9 Change of refractive index and thickness during the reduction at –0.097 V in the pH 2.3 sulfate solution for the passive film formed at potential of 1.11 V.

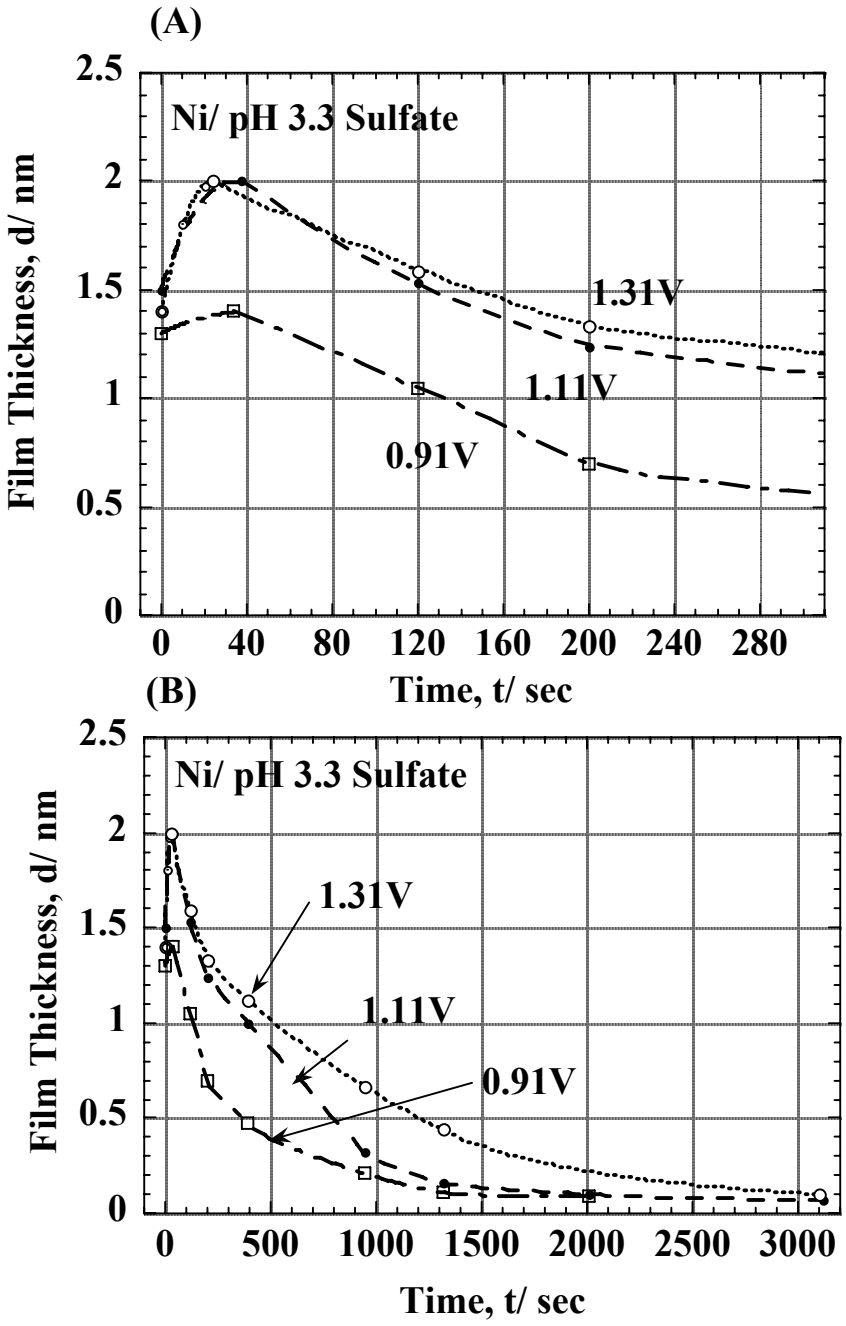

Figure 10 Change of thickness during the reduction at –0.108 V in the pH 3.3 sulfate solution for the passive film formed at potentials of 0.91, 1.11, and 1.31 V.